Coordinate-independent angle-gathers for wave equation migration

Paul Sava and Sergey Fomel, Bureau of Economic Geology, The University of Texas at Austin

SUMMARY

We formulate angle decomposition, during and after wavefield extrapolation, independent of the choice of coordinate systems. The key idea is to describe the source-receiver separation during wavefield extrapolation as a vector quantity. This formulation links the reflection angle to the magnitude of the offset vector, thus reducing the cost and storage associated with angle decomposition. This coordinate-independent formulation eliminates the difficulties encountered by traditional angle decompositions for steeply dipping reflectors, and it can also be used for extrapolation techniques in general, non-Cartesian coordinate systems.

INTRODUCTION

Migration by downward continuation can accurately image complex geological structures. Wavefield extrapolation compares favorably with direct methods, such as Kirchhoff migration, for its ability to handle multi-pathing, strong velocity heterogeneities, and finite-bandwidth wave-propagation effects (Gray et al., 2001).

However, migration by downward continuation imposes limitations on the dip of reflectors that can be imaged since it favors energy that is propagating mainly in the downward direction. Upward propagating energy, e.g., overturning waves, can be imaged in principle using downward continuation methods (Hale et al., 1992), although the procedure is difficult, particularly for prestack data. In contrast, Kirchhoff-type methods based on ray-traced traveltimes can image steep dips and handle overturning waves, although those methods are far less reliable in complex environments given their high-frequency asymptotic nature.

Several options proposed recently alleviate the limitations imposed by downward continuation. Among those methods are techniques that increase the angular accuracy of the extrapolation operators, (Ristow and Ruhl, 1994; Biondi, 2002; de Hoop, 1996; Huang and Wu, 1996), techniques that use extrapolation in tilted coordinates (Etgen, 2002; Shan and Biondi, 2004), or hybrid ray-wavefield methods (Cervený, 2001; Hill, 2001; Brandsberg-Dahl and Etgen, 2003; Sava and Fomel, 2004).

Velocity and amplitude information can be extracted from depth migrated images using wavefield extrapolation using techniques that decompose the imaged data into angle-dependent components (de Bruin et al., 1990; Prucha et al., 1999; Mosher and Foster, 2000; Rickett and Sava, 2002; Xie and Wu, 2002; Sava and Fomel, 2003; Soubaras, 2003; Biondi and Symes, 2004). The key element for imaging in the angle domain is the imaging condition that must preserve the effective offset relating the sources and receivers during extrapolation. The usual procedure is to employ the horizontal component of this offset vector, but this approach has difficulties when imaging steeply dipping reflectors for which the horizontal projection of the offset vector vanishes. One way of addressing this problem is to compute the vertical component of the offset vector (Biondi and Shan, 2002; Biondi and Symes, 2004). However, even this approach is limited in that it requires storage of various components of the offset vector as well as selection of the imaging option depending on the local structure.

In this paper, we demonstrate that the angle transformations can be formulated independent of the coordinate system in which we solve the imaging problem. The key technical element of our method is that we formulate it using vector source-receiver offsets. In this way, the angle decomposition is independent of any particular discretization, thus it can be used for wavefields extrapolated in non-Cartesian coordinate systems, e.g. using Riemannian wavefield extrapolation (Sava and Fomel, 2004).

SPACE-DOMAIN IMAGING CONDITION

A traditional imaging condition for shot-record migration, also known as UD^* imaging condition (Claerbout, 1985), can be written as:

$$\mathbf{R}_0(\mathbf{m}) = \sum_{\omega} \mathbf{U}_s(\mathbf{m},\omega)\,\mathbf{U}_r{}^*(\mathbf{m},\omega)\ , \tag{1}$$

where $\mathbf{U}_s$ is the source wavefield, $\mathbf{U}_r$ is the receiver wavefield, $\mathbf{m} = [m_x, m_y, m_z]$ is a vector describing the locations of image points, and ω stands for temporal frequency. The summation over frequencies ω extracts the image $\mathbf{R}$ at zero time. m_x and m_y are the horizontal coordinates, and m_z is the depth coordinate of an image point relative to a reference coordinate system.

We propose a generalized imaging condition by which reflectivity is estimated using the expression

$$\mathbf{R}(\mathbf{m},\mathbf{h}) = \sum_{\omega} \mathbf{U}_s(\mathbf{m}-\mathbf{h},\omega)\,\mathbf{U}_r{}^*(\mathbf{m}+\mathbf{h},\omega)\ , \tag{2}$$

where $\mathbf{h} = [h_x, h_y, h_z]$ is a vector describing the local source-receiver separation in the image space. This imaging condition reveals data that are not mapped to zero-offset in the imaging process, indicating velocity inaccuracies and allowing angle-domain decompositions of the migrated images. The components of the $\mathbf{h}$ vectors are the two conventional horizontal offsets, h_x and h_y (Rickett and Sava, 2002), and a vertical offset h_z (Biondi and Symes, 2004).

Migration velocity analysis and reflectivity versus angle analysis requires image decomposition function of angles at every location

$$\mathbf{R}(\mathbf{m},\mathbf{h}) \Longrightarrow \mathbf{R}(\mathbf{m},\theta,\phi)\ , \tag{3}$$

where θ is the incidence angle made by the source ray with the normal to the reflector, and ϕ is the azimuth of the reflection plane measured relative to a conventional reference (Figure 1).

REFLECTION ANGLE (θ)

Using the definitions introduced in the preceding section, we can make the standard notations for the source and receiver coordinates: $\mathbf{s} = \mathbf{m} - \mathbf{h}$ and $\mathbf{r} = \mathbf{m} + \mathbf{h}$. The traveltime from a source to a receiver is a function of all spatial coordinates of the seismic experiment $t = t(\mathbf{m},\mathbf{h})$. Differentiating t with respect to all components of the vectors $\mathbf{m}$ and $\mathbf{h}$, and using the standard notations $\mathbf{p}_\alpha = \nabla_\alpha t$, where $\alpha = \{\mathbf{m},\mathbf{h},\mathbf{s},\mathbf{r}\}$, we can write:

$$\mathbf{p_m} = \mathbf{p_r} + \mathbf{p_s}\ , \tag{4}$$

$$\mathbf{p_h} = \mathbf{p_r} - \mathbf{p_s}\ . \tag{5}$$

By analyzing the geometric relations of various vectors at an image point (Figure 1), we can write the following trigonometric expressions:

$$|\mathbf{p_h}|^2 = |\mathbf{p_s}|^2 + |\mathbf{p_r}|^2 - 2|\mathbf{p_s}||\mathbf{p_r}|\cos(2\theta)\ , \tag{6}$$

$$|\mathbf{p_m}|^2 = |\mathbf{p_s}|^2 + |\mathbf{p_r}|^2 + 2|\mathbf{p_s}||\mathbf{p_r}|\cos(2\theta)\ , \tag{7}$$

$$\mathbf{p_m}\cdot\mathbf{p_h} = |\mathbf{p_r}|^2 - |\mathbf{p_s}|^2\ . \tag{8}$$

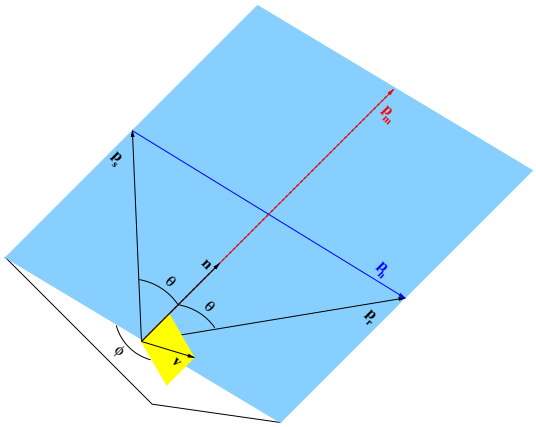

Figure 1: Geometric relations between ray vectors at a reflection point.

Defining $\mathbf{k_m}$ and $\mathbf{k_h}$ as the location and offset wavenumber vectors, we can replace $|\mathbf{p_m}| = |\mathbf{k_m}|/\omega$ and $|\mathbf{p_h}| = |\mathbf{k_h}|/\omega$. Using the trigonometric identity

$$\cos(2\theta) = \frac{1-\tan^2\theta}{1+\tan^2\theta} \; , \tag{9}$$

and assuming $|\mathbf{p_s}| = |\mathbf{p_r}| = s$, where $s(\mathbf{m})$ is the slowness at an image location, we obtain the following relations:

$$|\mathbf{k_h}|^2 = (2\omega s)^2 \frac{\tan^2\theta}{1+\tan^2\theta} \; , \tag{10}$$

$$|\mathbf{k_m}|^2 = (2\omega s)^2 \frac{1}{1+\tan^2\theta} \; , \tag{11}$$

$$\mathbf{k_m} \cdot \mathbf{k_h} = 0 \; . \tag{12}$$

Equations (10)-(12) can be used for angle decomposition in various imaging scenarios, as described in the following sections. Those expressions depend on 6 components of the space and offset vectors, $\mathbf{m}$ and $\mathbf{h}$, and on frequency ω and slowness $s(\mathbf{m})$. An analogous analysis for converted waves, when $|\mathbf{p_s}| \neq |\mathbf{p_r}|$, is presented by Sava and Fomel (2005).

Angle-decomposition after imaging

We can eliminate from equations (10)-(12) the dependence on frequency and slowness, and obtain an angle decomposition formulation prior to imaging. Solving for $\tan\theta$, we obtain an expression for the reflection angle function of position and offset wavenumbers $(\mathbf{k_m}, \mathbf{k_h})$:

$$\boxed{\tan\theta = \frac{|\mathbf{k_h}|}{|\mathbf{k_m}|} \; .} \tag{13}$$

Formulation (13) is independent of the coordinate system in which we define the imaging problem, and thus it could be used for Riemannian wavefield extrapolation (Sava and Fomel, 2004).

If we express the vectors $\mathbf{k_m}$ and $\mathbf{k_h}$ using their components in an arbitrary Cartesian coordinate system, we can rewrite equations (12) and (13)

$$\tan^2\theta = \frac{k_{h_x}^2 + k_{h_y}^2 + k_{h_z}^2}{k_{m_x}^2 + k_{m_y}^2 + k_{m_z}^2} \; , \tag{14}$$

$$0 = k_{m_x} k_{h_x} + k_{m_y} k_{h_y} + k_{m_z} k_{h_z} \; . \tag{15}$$

We can consider one special situation when we eliminate the dependency on the vertical offset from the system (14)-(15). If we substitute k_{h_z} from equation (15)

$$k_{h_z} = -k_{h_x}\frac{k_{m_x}}{k_{m_z}} - k_{h_y}\frac{k_{m_y}}{k_{m_z}} \tag{16}$$

into equation (14), we obtain the 3-D angle-gather transformation formula of Fomel (2004):

$$\tan^2\theta = \frac{k_{m_z}^2 (k_{h_x}^2 + k_{h_y}^2) + (k_{h_x} k_{m_x} + k_{h_y} k_{m_y})^2}{k_{m_z}^2 (k_{m_x}^2 + k_{m_y}^2 + k_{m_z}^2)} \; . \tag{17}$$

Under the common-azimuth approximation, this expression reduces to (Biondi and Symes, 2004)

$$\tan^2\theta = \frac{k_{h_x}^2}{k_{m_y}^2 + k_{m_z}^2} \; , \tag{18}$$

and for 2-D data or purely inline reflections, this expression reduces to (Sava and Fomel, 2003)

$$\tan\theta = \frac{k_{h_x}}{k_{m_z}} \; . \tag{19}$$

Another possibility is to eliminate one spatial wavenumber, but preserve the vertical offset. For example, we can substitute k_{m_x} from equation (15) into equation (14) and obtain the relation

$$\tan^2\theta = \frac{k_{h_x}^2 \left(k_{h_x}^2 + k_{h_y}^2 + k_{h_z}^2\right)}{k_{h_x}^2 \left(k_{m_y}^2 + k_{m_z}^2\right) + \left(k_{h_y} k_{m_y} + k_{h_z} k_{m_z}\right)^2} \; . \tag{20}$$

Under the common-azimuth approximation, that implies $\frac{k_{h_z}}{k_{m_z}} = \frac{k_{h_y}}{k_{m_y}}$, this expression also reduces to equation (18).

Angle decomposition before imaging

We can eliminate from equations (10)-(12) the dependence on depth and obtain an angle decomposition formulation prior to imaging. If we eliminate k_{m_z} and k_{h_z} from equations (14) and (15), we obtain the expression (Fomel, 2004):

$$\left(k_{m_x}^2 + k_{m_y}^2\right)(2\omega s \sin\theta)^2 + \left(k_{h_x}^2 + k_{h_y}^2\right)(2\omega s \cos\theta)^2 = \left(k_{m_x} k_{h_y} - k_{m_y} k_{h_x}\right)^2 + (2\omega s \sin\theta)^2 (2\omega s \cos\theta)^2 \; . \tag{21}$$

The quadratic equation (21) can be used to map data from local offset gathers $\{k_{h_x}, k_{h_y}\}$ into angle coordinates $s\sin\theta$, function of the temporal frequency ω, prior to imaging For 2-D data, equation (21) takes the simpler form

$$k_{m_x}^2 (2\omega s \sin\theta)^2 + k_{h_x}^2 (2\omega s \cos\theta)^2 = (2\omega s \sin\theta)^2 (2\omega s \cos\theta)^2 \; , \tag{22}$$

which can be solved for an explicit mapping of k_{h_x} to $s\sin\theta$.

AZIMUTH ANGLE (ϕ)

We can define an azimuth reference using a vector included in the reflecting plane. For this purpose, we need to introduce $\mathbf{v}$ as an arbitrary vector (e.g. pointing North), and $\mathbf{n}$ as the vector normal to the reflecting plane. Then, the vector product $\mathbf{v} \times \mathbf{n}$ is a vector that is contained in the reflecting plane and defines a reference azimuth according to a fixed direction, and the local dip of the reflecting plane. Similarly, the

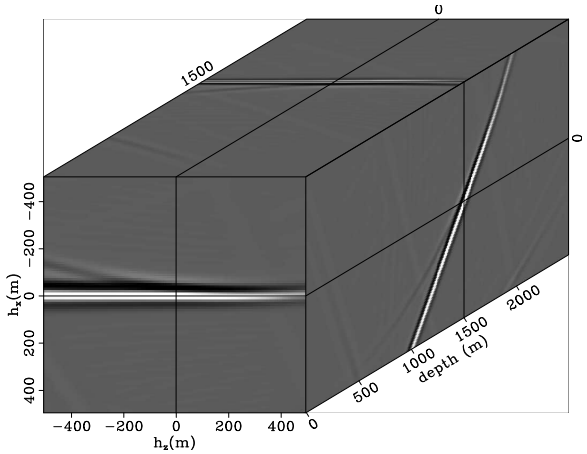

Figure 2: Multi-offset common-image gather for a flat reflector.

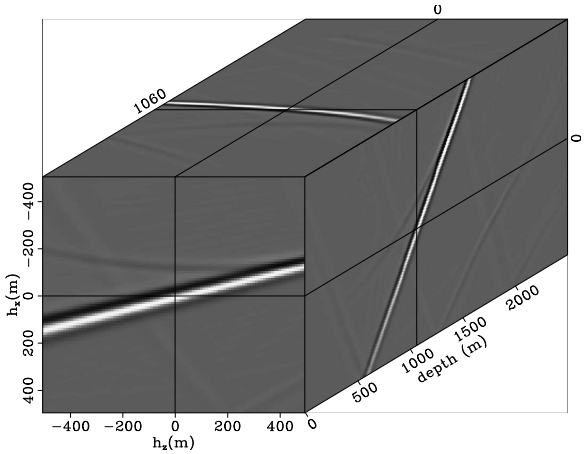

Figure 3: Multi-offset common-image gather for a dipping reflector.

vector product $\mathbf{p_h} \times \mathbf{p_m}$ is a vector contained in the reflecting plane that rotates 360° with the azimuth of the reflection plane.

Then, the azimuth between the vectors $\mathbf{v} \times \mathbf{n}$ and $\mathbf{p_h} \times \mathbf{p_m}$ is simply defined by the expression:

$$\cos\phi = \frac{(\mathbf{v}\times\mathbf{n})\cdot(\mathbf{p_h}\times\mathbf{p_m})}{|\mathbf{v}\times\mathbf{n}||\mathbf{p_h}\times\mathbf{p_m}|} \ , \tag{23}$$

or, using the vectors $\mathbf{k_m}$ and $\mathbf{k_h}$ by the expression:

$$\boxed{\cos\phi = \frac{(\mathbf{v}\times\mathbf{n})\cdot(\mathbf{k_h}\times\mathbf{k_m})}{|\mathbf{v}\times\mathbf{n}||\mathbf{k_h}\times\mathbf{k_m}|} \ .} \tag{24}$$

For P-P reflections, vector $\mathbf{n}$ is aligned with vector $\mathbf{k_m}$.

FOURIER-DOMAIN IMAGING CONDITION

The imaging condition (2) can also be formulated in the Fourier domain similarly to the approach of Artman and Fomel (2005). In the Fourier domain, we can write

$$\widehat{\widehat{\mathbf{R}}}(\mathbf{k_m},\mathbf{k_h}) = \frac{1}{2}\sum_{\omega}\widehat{\mathbf{U}_s}\left(\frac{\mathbf{k_m}-\mathbf{k_h}}{2},\omega\right)\widehat{\mathbf{U}_r}^{*}\left(\frac{\mathbf{k_m}+\mathbf{k_h}}{2},\omega\right) \ , \tag{25}$$

where $\widehat{\ }$ stands for a Fourier transform, and * for complex conjugate. The image $\mathbf{R}_0$ is obtained using an inverse Fourier transform over $\mathbf{k_m}$ of the image constructed using equation (25), after summation over the offset wavenumbers $|\mathbf{k_h}|$:

$$\mathbf{R}_0(\mathbf{m}) = \mathtt{IFT}\sum_{|\mathbf{k_h}|}\widehat{\widehat{\mathbf{R}}}(\mathbf{k_m},\mathbf{k_h}) \ . \tag{26}$$

An intriguing possibility is raised by the following construction: the image constructed using equation (25) is formulated in the $\mathbf{k_m},\mathbf{k_h}$ Fourier domain; the angle-mapping formula (13) is also written in the Fourier domain; therefore, using equations (25) and (13), we can construct a second image based on the following formula:

$$\widehat{\widehat{\mathbf{R}}}_\theta(\mathbf{k_m},\mathbf{k_h}) = \widehat{\widehat{\mathbf{R}}}(\mathbf{k_m},\mathbf{k_h})\,\frac{|\mathbf{k_h}|}{|\mathbf{k_m}|} \ . \tag{27}$$

This image can also be transformed to the space domain using summation over the offset wavenumbers $|\mathbf{k_h}|$ and inverse Fourier transform over the space coordinates

$$\mathbf{R}_\theta(\mathbf{m}) = \mathtt{IFT}\sum_{|\mathbf{k_h}|}\widehat{\widehat{\mathbf{R}}}_\theta(\mathbf{k_m},\mathbf{k_h}) \ . \tag{28}$$

Then, using equations (26) and (28), we can obtain the reflection angle field $\tan\theta(\mathbf{m})$ using a simple division of the two images:

$$\tan\theta(\mathbf{m}) = \frac{\mathbf{R}_\theta(\mathbf{m})}{\mathbf{R}_0(\mathbf{m})} \ , \tag{29}$$

analogously to methodology employed by Bleistein et al. (2000) to Kirchhoff imaging. The reflection angle field $\tan\theta(\mathbf{m})$ describes the angle at which one particular shot illuminates the image $\mathbf{R}_0(\mathbf{m})$. The final image is obtained by summation of all such images constructed for independent shots, with contribution of different shots added at their respective angle. This approach substantially reduces the storage requirements for shot-record migration, while still producing angle-dependent reflectivity. A similar procedure can be used to encode the reflection azimuth field $\cos\phi(\mathbf{m})$ instead of the reflection angle field $\tan\theta(\mathbf{m})$, by using equation (24) as the scale factor in equation (27).

EXAMPLE

Figures 2 and 3 illustrate the importance of the vertical offset in angle-gather transformations. The two figures correspond to flat and dipping reflectors, respectively. The front two axes are horizontal and vertical offsets, h_x and h_z, and the third axis is depth. For the flat reflector, $h_z = const$, but for the dipping reflector, $h_z \neq const$. For the later case, reconstructing the offset wavenumber vector used in equation (13) requires computation of all three components of the vector.

Figures 4 and 5 show common-image gathers using absolute offsets instead of the more common horizontal offsets. The left panels in both figures are offset-domain image gathers. Although corresponding to flat and dipping reflectors, the offset gathers show, as expected, identical moveouts. Since we are operating with absolute offsets, both the positive and the negative cross-correlation lags are present in the image gather, but with opposite dips. Mapping to the angle-domain produces equivalent gathers, as shown in the right panels of Figures 4 and 5.

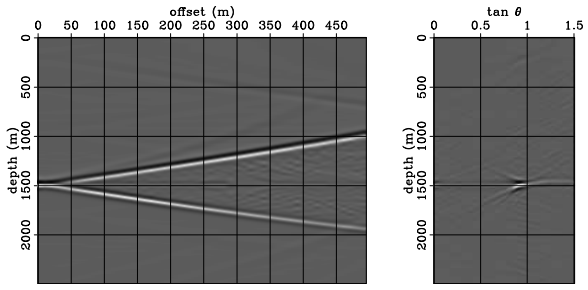

Figure 4: Full offset gather for a flat reflector and its conversion to angle.

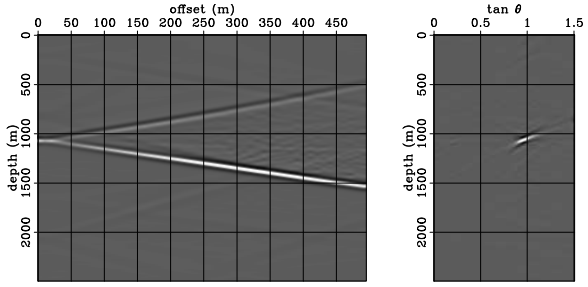

Figure 5: Full offset gather for a dipping reflector and its conversion to angle.

CONCLUSION

We implement coordinate-independent angle decomposition for images constructed using migration by wavefield extrapolation. This transformation involves computing 3-D offset vectors **h** during the imaging step. This requirement adds more computations, since more cross-correlations are required. However, the storage requirements for reflection angle imaging is decreased, since the transformation depends on the absolute magnitude of the offset vector ($|\mathbf{k_h}| = k_{|\mathbf{h}|}$), rather than on its components. Azimuth analysis requires storage of all offset vector components.

REFERENCES

Artman, B., and Fomel, S., 2005, Fourier domain imaging condition for shot-profile migration *in* 75th Ann. Internat. Mtg. Soc. of Expl. Geophys.

Biondi, B., 2002, Stable wide-angle Fourier finite-difference downward extrapolation of 3-D wavefields: Geophysics, **67**, 872–882.

Biondi, B., and Shan, G., 2002, Prestack imaging of overturned reflections by reverse time migration *in* 72nd Ann. Internat. Mtg. Soc. of Expl. Geophys., 1284–1287.

Biondi, B., and Symes, W. W., 2004, Angle-domain common-image gathers for migration velocity analysis by wavefield-continuation imaging: Geophysics, **69**, 1283–1298.

Bleistein, N., Cohen, J., and Stockwell, J., 2000, Mathematics of multidimensional seismic imaging, migration, and inversion: Springer.

Brandsberg-Dahl, S., and Etgen, J., 2003, Beam-wave migration: 65th Mtg., Eur. Assoc. Geosc. Eng., Abstracts.

de Bruin, C. G. M., Wapenaar, C. P. A., and Berkhout, A. J., 1990, Angle-dependent reflectivity by means of prestack migration: Geophysics, **55**, 1223–1234.

Cervený, V., 2001, Seismic ray theory: Cambridge Univ. Press.

Claerbout, J. F., 1985, Imaging the Earth's Interior: Blackwell Scientific Publications.

Etgen, J., 2002, Waves, beams and dimensions: an illuminating if incoherent view of the future of migration: 72nd Ann. Internat. Mtg, Soc. of Expl. Geophys.

Fomel, S., 2004, Theory of 3-D angle gathers in wave-equation imaging *in* 74th Ann. Internat. Mtg. Soc. of Expl. Geophys.

Gray, S. H., Etgen, J., Dellinger, J., and Whitmore, D., 2001, Seismic migration problems and solutions: Geophysics, **66**, 1622–1640.

Hale, D., Hill, N. R., and Stefani, J., 1992, Imaging salt with turning seismic waves: Geophysics, **57**, 1453–1462.

Hill, N. R., 2001, Prestack Gaussian-beam depth migration: Geophysics, **66**, 1240–1250.

de Hoop, M. V., 1996, Generalization of the Bremmer coupling series *in* J. Math. Phys. 3246–3282.

Huang, L. Y., and Wu, R. S., 1996, Prestack depth migration with acoustic screen propagators *in* 66th Ann. Internat. Mtg. Soc. of Expl. Geophys., 415–418.

Mosher, C., and Foster, D., 2000, Common angle imaging conditions for prestack depth migration *in* 70th Ann. Internat. Mtg. Soc. of Expl. Geophys., 830–833.

Prucha, M., Biondi, B., and Symes, W., 1999, Angle-domain common image gathers by wave-equation migration *in* 69th Ann. Internat. Mtg. Soc. of Expl. Geophys., 824–827.

Rickett, J. E., and Sava, P. C., 2002, Offset and angle-domain common image-point gathers for shot-profile migration: Geophysics, **67**, 883–889.

Ristow, D., and Ruhl, T., 1994, Fourier finite-difference migration: Geophysics, **59**, 1882–1893.

Sava, P., and Fomel, S., 2004, Riemannian wavefield extrapolation *in* 74th Ann. Internat. Mtg. Soc. of Expl. Geophys.

—, 2005, Wave-equation common-angle gathers for converted waves *in* 75th Ann. Internat. Mtg. Soc. of Expl. Geophys.

Sava, P. C., and Fomel, S., 2003, Angle-domain common-image gathers by wavefield continuation methods: Geophysics, **68**, 1065–1074.

Shan, G., and Biondi, B., 2004, Imaging overturned waves by plane-wave migration in tilted coordinates: SEG Technical Program Expanded Abstracts, **23**, 969–972.

Soubaras, R., 2003, Angle gathers for shot-record migration by local harmonic decomposition *in* 73rd Ann. Internat. Mtg. Soc. of Expl. Geophys., 889–892.

Xie, X., and Wu, R., 2002, Extracting angle domain information from migrated wavefield *in* 72nd Ann. Internat. Mtg. Soc. of Expl. Geophys., 1360–1363.